Investigation of Thermally Conducting Phase-Change Materials Based on Polyethylene/Wax Blends Filled with Copper Particles

J. A. Molefi,[1] A. S. Luyt,[1] I. Krupa[2]

[1]*Department of Chemistry, University of the Free State (Qwaqwa Campus), Private Bag X13, Phuthaditjhaba, 9866, South Africa*
[2]*Polymer Institute, Slovak Academy of Sciences, 842 36 Bratislava, Slovak Republic*

Received 17 July 2009; accepted 21 October 2009
DOI 10.1002/app.31653
Published online 5 January 2010 in Wiley InterScience (www.interscience.wiley.com).

ABSTRACT: This article reports on the morphology, melting and crystallization behavior, thermal stability, tensile properties, and thermal conductivity of phase-change materials (PCM) for thermal energy storage. These materials were based on a soft Fischer-Tropsch paraffin wax (PCM) blended with low-density polyethylene, linear low-density polyethylene, and high-density polyethylene. These immiscible blends were melt-mixed with copper (Cu) microparticles (up to 15 vol %) to improve the thermal conductivity in the matrix material. The presence of the Cu microparticles in the PCMs did not significantly change the crystallization behavior, thermal stability, or tensile properties of the blend composites in comparison with the corresponding polyethylene/wax blends and polyethylene/Cu composites. The observed differences were related to the fact that the wax seemed to have a higher affinity for the Cu particles than any of the polyethylenes, and so it crystallized as a layer around the Cu particles. The thermal conductivity of the samples increased almost linearly with increasing Cu content, but the samples had slightly lower values than the corresponding polyethylene/Cu composites, probably because of the lower thermal conductivity of the wax. © 2010 Wiley Periodicals, Inc. J Appl Polym Sci 116: 1766–1774, 2010

Key words: blends; composites; differential scanning calorimetry (DSC); morphology; polyethylene (PE)

INTRODUCTION

Phase-change materials (PCMs) are substances with a high heat of fusion that, through melting and solidification at certain temperatures, are capable of storing or releasing large amounts of energy.[1,2] PCMs have received a lot of interest for many applications such as energy storage and thermal protection systems and for the active and passive cooling of electronic devices.[3] For use in active and passive cooling applications, PCMs should possess high thermal conductivity to meet the required heat exchange rates.[4,5] Moreover, these materials should have a small volume change and low degrees of supercooling. It is therefore challenging to find an ideal PCM that satisfies all the desirable properties. Different inorganic and organic substances have already been used for the creation of PCMs; paraffin waxes are among those with the greatest prospects.[6]

Paraffin waxes are used as PCMs for thermal storage applications because of their desirable characteristics, such as a high latent heat of fusion, negligible supercooling, a low vapor pressure in the melt, chemical inertness and stability, self-nucleation, no phase segregation, and commercial availability at a low cost. However, waxes exhibit some inherent limitations, such as low thermal conductivity and a large volume change during a phase transition.[7] When paraffin waxes are used in energy-storage systems, their lower thermal conductivity reduces the heat exchange rate during melting and solidification cycles, and so the overall power of the phase-change regenerator decreases. Paraffin waxes, blended with appropriate polymers, seem to be the best candidates for the preparation of smart polymeric PCMs for different applications such as the thermal storage of solar energy, thermal protection of electronic devices, thermal protection of food and medical goods, passive storage in bioclimatic buildings, use of off-peak rates, reduction of installed power, and thermal comfort in vehicles.[8–10]

Correspondence to: A. S. Luyt (luytas@qwa.ufs.ac.za).
Contract grant sponsor: National Research Foundation of South Africa; contract grant number: GUN 62693.
Contract grant sponsor: University of the Free State.
Contract grant sponsor: Scientific Grant Agency of the Ministry of Education of the Slovak Republic.
Contract grant sponsor: Slovak Academy of Sciences; contract grant number: 2/0063/09.

To improve the thermal conductivity of PCMs, they have been blended with various inorganic fillers. Among the commonly used fillers are graphite and expanded graphite,[11,12] carbon nanotubes,[13] aluminum nitride,[14] and various types of metallic particles.[15]

Polyethylene (PE) seems to be the polymer most frequently used for blending with paraffin waxes to obtain PCMs because of the good compatibility of both components.[16–20] However, our previous results have indicated some potential problems concerning PE/paraffin wax blends[21–23] associated with the phase separation of the components. They indicate the necessity of carefully selecting polymer/paraffin wax blends and the need for determining the morphology and phase behavior of the investigated materials. Characterization based on differential scanning calorimetry (DSC) measurements alone is not sufficient. Very recently, we discussed the thermal and morphological stability of PE and polypropylene blended with paraffin wax. The dynamic mechanical analyses of the blends pointed out an important aspect that in most cases is neglected. It is always a question of which component forms the continuous phase and which forms the discontinuous phase. Even though the highest concentration of paraffin wax used to form a low-density polyethylene (LDPE) continuous phase was set at 50 wt %, it was still not enough to keep the material structure in a consistent shape. Controlled-force ramp testing in dynamic mechanical analysis confirmed the poor material strength, especially at temperatures above the wax melting temperature, that is, temperatures that are interesting for energy-storage applications. The highest paraffin wax concentration able to sustain the external forces and the thermal cycling was 40 wt %.[24,25]

This article reports on the morphology, melting and crystallization behavior, thermal stability, tensile properties, and thermal conductivity of PCMs based on various types of PEs blended with soft Fischer-Tropsch paraffin wax. The thermal conductivity of the materials was improved by the addition of microsized and nanosized copper (Cu) particles.

EXPERIMENTAL

Materials and sample preparation

In this work, LDPE and linear low-density polyethylene (LLDPE) were supplied in pellet form by Sasol Polymers (Johannesburg, South Africa). The LDPE had a melt flow index (MFI) of 7.0 g/10 min (ASTM D 1238), a melting point of 106°C, a molecular weight of 96,000 g/mol, and a density of 0.918 g/cm^3; the LLDPE had an MFI of 1.0 g/10 min (ASTM D 1238), a molecular weight of 191,600 g/mol, a melting point of 124°C, and a density of 0.924 g/cm^3. High-density polyethylene (HDPE) was supplied in pellet form by Dow Chemicals. It had an MFI of 8 g/10 min (ASTM D 1238), a molecular weight of 168,000 g/mol, a melting point of 130°C, and a density of 0.954 g/cm^3. Soft paraffin wax (M3 wax) was supplied in powder form by Sasol Wax. It had an average molar mass of 440 g/mol and a carbon distribution between C15 and C78. Its density was 0.90 g/cm^3, and it had a melting point range of approximately 40–60°C. Merck Chemicals (South Africa) supplied the Cu powder, which was used as one of the conducting fillers. It had a melting point of 1083°C and a density of 8.96 g/cm^3, and the particle sizes were less than 38 μm (as determined with a laboratory test sieve with a pore size of 38 μm).

All the samples were prepared through the mixing of the components in a Brabender Plastograph 50-mL internal mixer at 160°C and a speed of 70 rpm for 15 min. After the mixing, the samples were melt-pressed at 100 bar and 160°C for 15 min.

Sample characterization and analysis

A Shimadzu (Kyoto, Japan) Superscan ZU SSX-550 scanning electron microscope was used for the scanning electron microscopy (SEM) analyses. All samples were frozen in liquid nitrogen, simply fractured to an appropriate size to fit within the specimen chamber, and then mounted onto the holder. The surfaces of the samples were coated with gold by an electrodeposition method to impart electrical conduction before the SEM micrographs were recorded. This was done to prevent the accumulation of static electric charge on the specimens during electron irradiation.

DSC analyses were done in a PerkinElmer (Wellesley, MA) Pyris-1 differential scanning calorimeter under flowing nitrogen (flow rate = 20 mL/min). The instrument was computer-controlled, and the peak analyses were done with Pyris software. The instrument was calibrated with the onset temperatures of melting of indium and zinc standards as well as the melting enthalpy of indium. Samples (5–10 mg) were sealed in aluminum pans, heated from −40 to 160°C at a heating rate of 10°C/min, and cooled at the same rate. For the second scan, the samples were heated and cooled under the same conditions. The peak temperatures of melting and crystallization, as well as the melting and crystallization enthalpies, were determined from the second scan. All DSC measurements were repeated three times for each sample. The temperatures and enthalpies are reported as average values with standard deviations.

Thermogravimetric analysis (TGA) was carried out in a PerkinElmer TGA7 thermogravimetric analyzer. Samples (5–10 mg) were heated from 30 to

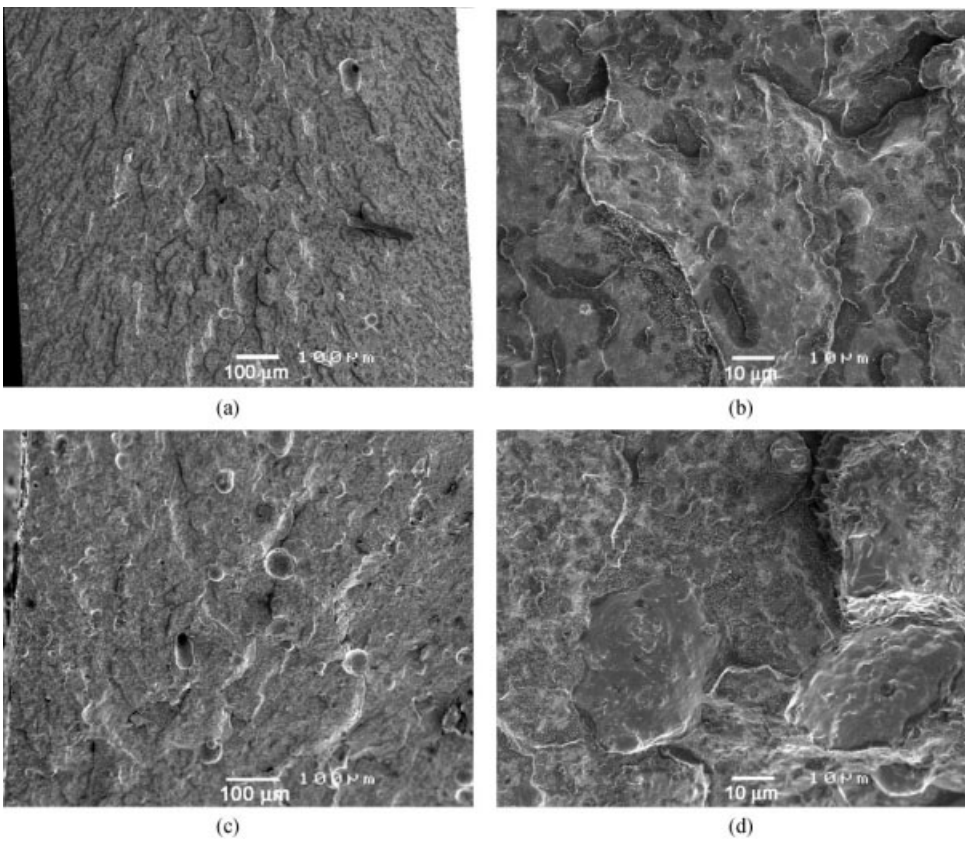

Figure 1 SEM images of the (a) 59/40/1 v/v LDPE/wax/Cu microcomposite (low magnification), (b) 59/40/1 v/v LDPE/wax/Cu microcomposite (high magnification), (c) 55/40/5 v/v LDPE/wax/Cu microcomposite (low magnification), and (d) 55/40/5 v/v LDPE/wax/Cu microcomposite (high magnification).

650°C at a heating rate of 20°C/min under flowing nitrogen (flow rate = 20 mL/min).

A Hounsfield (Redhill, England) H5KS universal testing machine was used for the tensile analysis of the samples. The dumbbell samples were stretched at a speed of 50 mm/min under a cell load of 250.0 N. The dumbbell samples had a total length of 75 mm, a gauge length of 24 mm, a neck width of 5 mm, and a thickness of 1 mm. About nine test samples were cut with a dumbbell cutter, and they were all tested. Stress–strain curves that indicated sample deficiencies were ignored during the final calculations of the tensile properties.

The thermal conductivity was measured with a Isomet multipurpose apparatus (Applied Precision, Bratislava, Slovakia) for nonsteady measurements of thermal properties. The thermal conductivity values were calculated automatically from the time dependence of the thermal flow in the material. Samples were melt-pressed into spherical (7-cm-diameter), 1-mm-thick sheets in a hot-melt press at 160°C for 5 min at a pressure of 100 bar. Thereafter, measurements were made at 25 ± 2°C with a flat probe.

RESULTS AND DISCUSSION

SEM

Figure 1 shows SEM pictures of the fractured surfaces of LDPE/wax/Cu composites containing 1 or 5 vol % Cu powder and 40 vol % wax. The composites in all the pictures showed a two-phase morphology, which implied the immiscibility of LDPE and wax. Figure 1(a,c) shows fairly evenly distributed round holes where the spherical Cu particles dislodged during the cryofracturing of the composite samples. The differences in the Cu particle sizes are also evident, especially in Figure 1(c). Figure 1(d) very nicely shows a Cu particle with a diameter of about 30 µm embedded in the blend matrix and about an equally sized hole left by a dislodged Cu particle. The visible particle in Figure 1(d) was clearly covered by a wax layer, and this indicates that the Cu particles had a higher affinity for the wax. This preferable crystallization of the wax onto the Cu particles was probably the result of the incompatibility of the wax and the PEs as well as the thermodynamically more preferred adsorption of the smaller wax molecules onto the rough Cu surfaces.

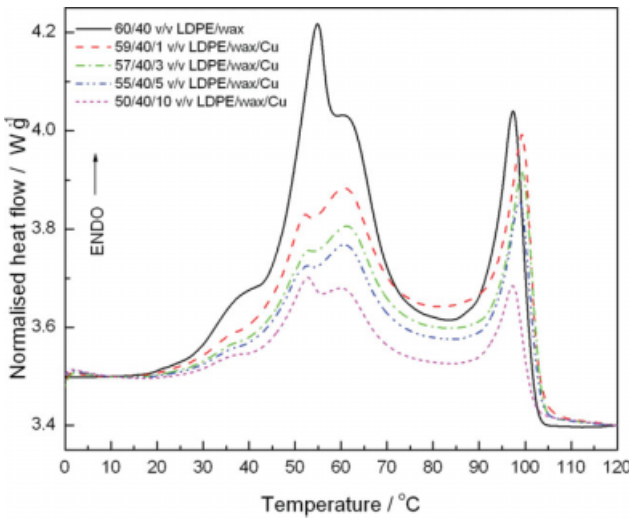

Figure 2 DSC heating curves of the LDPE, wax, and LDPE/wax/Cu microcomposites. [Color figure can be viewed in the online issue, which is available at www.interscience.wiley.com.]

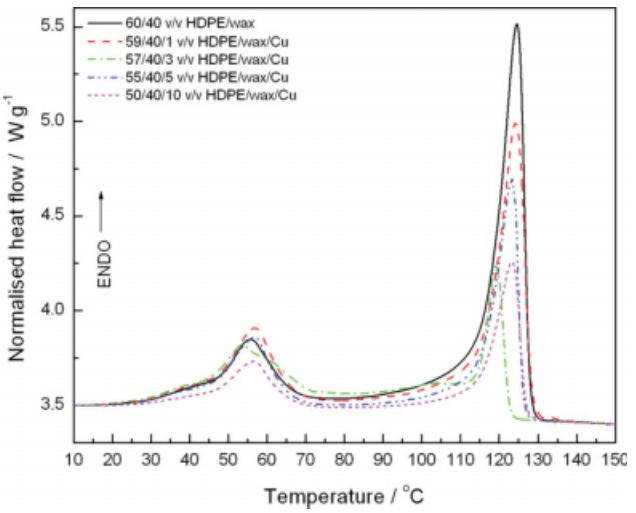

Figure 4 DSC heating curves of the HDPE, wax, and HDPE/wax/Cu microcomposites. [Color figure can be viewed in the online issue, which is available at www.interscience.wiley.com.]

DSC

The DSC heating curves of the PE/wax/Cu microcomposites are presented in Figures 2–4. The peak temperatures, as well as the melting and crystallization enthalpies, are summarized in Table I. This table also lists the enthalpies calculated according to the additive rule [eq. (1)]. An inspection of the figures and the tabulated values shows that the presence of Cu microparticles did not significantly change the thermal behavior of the PE/wax blends, even though the wax seemed to have a higher affinity for Cu and preferably crystallized on the Cu surface. The melting temperatures for the wax and all three polymers showed the same changes that were observed for the blends in the absence of Cu,[1] whereas the melting enthalpies in all cases corresponded well to those calculated according to the additive rule:

$$\Delta H_m^{\text{add}} = \Delta H_{m,\text{PE}} w_{\text{PE}} + \Delta H_{m,w} w_w \quad (1)$$

where $\Delta H_{m,\text{PE}}$, $\Delta H_{m,w}$, and $\Delta H_{\text{m}}^{\text{add}}$ are the specific enthalpies of melting of the PE, wax, and blends, respectively, and w_{PE} and w_w are the weight fractions of PE and wax in the blends, respectively. The relatively large experimental errors in the melting enthalpy values (standard deviations in Table I) indicated that the wax distribution in the different polymer matrices was fairly inhomogeneous. Because the Cu microparticles were primarily situated in the wax phase and because the presence of these particles did not seem to have changed the melting or crystallization behavior of the wax and/or the polymer, it was not possible to use the DSC results to support any conclusions made with respect to the Cu dispersion in any of the PE/wax blend matrices.

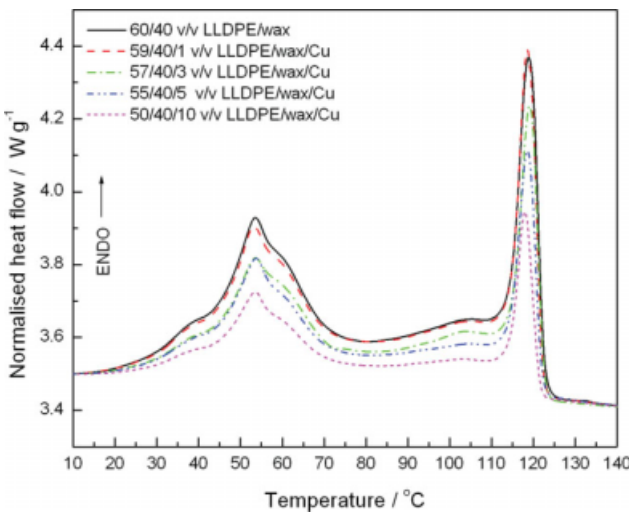

Figure 3 DSC heating curves of the LLDPE, wax, and LLDPE/wax/Cu microcomposites. [Color figure can be viewed in the online issue, which is available at www.interscience.wiley.com.]

TGA

The thermal stability results for the PE/wax/Cu microcomposites at a constant wax concentration of 40 vol % are presented in Figures 5–7 and are summarized in Table II. The composites degraded in two clearly distinguishable steps similar to those observed for the PE/wax blends.[26] The thermal stability of the composites generally increased with increasing Cu content, and it was higher than the thermal stability of the corresponding PE/wax

TABLE I
DSC Results for the PE/Wax/Cu Microcomposites

v/v	$T_{p,m}$ (°C)	ΔH_m^{obs} (J/g)	ΔH_m^{add} (J/g)	$T_{p,c}$ (°C)
LDPE/wax/Cu				
100/0/0	106.8 ± 1.5	75.4 ± 6.2	75.4	91.7 ± 0.6
60/40/0	55.5[a] ± 0.7	114.0 ± 10.9	113.6	55.8[a] ± 0.2
	96.9[b] ± 3.2			87.8[b] ± 1.8
59/40/1	58.1[a] ± 5.4	104.7 ± 6.8	104.0	55.6[a] ± 0.9
	99.9[b] ± 1.2			87.4[b] ± 0.9
57/40/3	61.3[a] ± 0.9	87.8 ± 3.4	88.0	55.8[a] ± 0.2
	100.6[b] ± 1.1			87.8[b] ± 1.8
55/40/5	60.6[a] ± 1.6	68.2 ± 9.0	79.3	56.0[a] ± 0.6
	99.3[b] ± 0.9			86.0[b] ± 0.5
50/40/10	53.2[a] ± 1.6	48.3 ± 4.0	56.5	53.8[a] ± 3.5
	98.4[b] ± 1.6			86.1[b] ± 0.5
0/100/0	58.4[a] ± 1.2	172.2 ± 0.1	172.2	53.1 ± 0.4
LLDPE/wax/Cu				
100/0/0	126.7 ± 2.1	86.9 ± 1.0	86.9	109.6 ± 0.9
60/40/0	54.5[a] ± 1.1	104.9 ± 15	120.6	49.8[a] ± 0.7
	119.8[b] ± 1.1			105.2[b] ± 1.1
59/40/1	54.9[a] ± 1.6	113.5 ± 6.6	109.5	49.8[a] ± 0.5
	120.4[b] ± 1.8			105.5[b] ± 0.8
57/40/3	54.7[a] ± 1.4	89.5 ± 10.4	92.5	49.8[a] ± 0.6
	120.6[b] ± 1.9			105.7[b] ± 0.8
55/40/5	54.6[a] ± 1.6	74.3 ± 9.5	80.4	50.1[a] ± 0.5
	119.9[b] ± 1.6			105.8[b] ± 0.8
50/40/10	55.1[a] ± 1.6	49.5 ± 12.0	59.6	50.1[a] ± 0.5
	120.0[b] ± 2.2			106.0[b] ± 1.0
0/100/0	58.4[a] ± 1.2	172.2 ± 0.1	172.2	53.1 ± 0.4
HDPE/wax/Cu				
100/0/0	134.7 ± 0.5	149.3 ± 9.7	149.3	113.9 ± 1.1
60/40/0	56.4[a] ± 0.4	153.2 ± 9.9	158.5	51.1[a] ± 0.6
	124.1[b] ± 2.3			110.2[b] ± 0.4
59/40/1	56.5[a] ± 0.6	150.0 ± 3.5	148.2	51.8[a] ± 1.1
	123.8[b] ± 0.7			109.2[b] ± 0.4
57/40/3	56.5[a] ± 0.4	113.7 ± 5.0	122.2	51.9[a] ± 0.6
	122.8[b] ± 0.4			109.7[b] ± 0.4
55/40/5	56.9[a] ± 0.4	91.7 ± 14.8	100.6	51.9[a] ± 0.6
	123.5[b] ± 0.2			110.1[b] ± 0.4
50/40/10	56.8[a] ± 0.1	77.1 ± 5.7	78.0	51.7[a] ± 0.1
	122.8[b] ± 1.0			110.1[b] ± 0.3
0/100/0	58.4[a] ± 1.2	172.2 ± 0.1	172.2	53.1 ± 0.4

$T_{p,m}$ = melting peak temperature; ΔH_m^{obs} = observed melting enthalpy; ΔH_m^{calc} = calculated melting enthalpy; $T_{p,c}$ = crystallization peak temperature.
[a] First peak maximum in the wax melting peak.
[b] Second peak maximum in the wax melting peak.

blends,[26] although this effect seemed to be less pronounced for the HDPE/wax/Cu microcomposites. The most likely reason for this observation was the higher crystallinity of HDPE, which gave rise to higher thermal stability in comparison with the other two PEs, even in the absence of Cu. In the presence of 10 vol % Cu, its thermal stability was comparable to that of the other two PEs. The higher thermal stability of all three PEs in the presence of Cu was probably due to the immobilization of PE and wax free radicals and volatile degradation products. There was a very good correlation between the residue weight percentage at 550°C and the weight percentage of Cu particles initially mixed into the sample. This indicated (1) the absence of any char formation during the thermal decomposition of the PE/wax/Cu conductive PCMs and (2) a fairly good dispersion of the Cu particles in the PE/wax matrix.

Tensile testing

Table III shows the tensile data for the PE/wax/Cu composites. The presence of Cu powder with a constant wax content caused an increase in the tensile strength for LDPE and LLDPE at low Cu contents, and this was followed by a decrease as the Cu content in the composites increased. The reason for the initial increase in the tensile strength is not clear, but

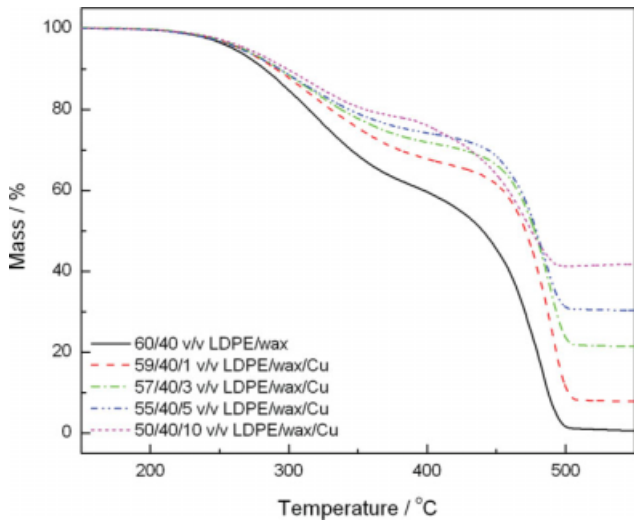

Figure 5 TGA curves for the LDPE, wax, and different LDPE/wax/Cu microcomposites. [Color figure can be viewed in the online issue, which is available at www.interscience.wiley.com.]

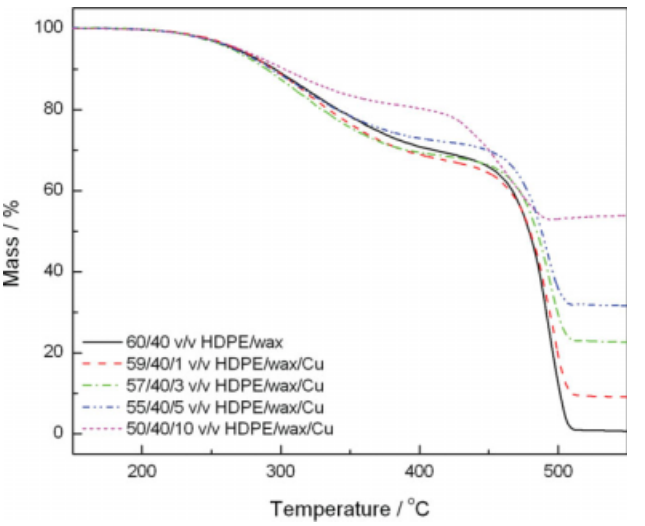

Figure 7 TGA curves for the HDPE, wax, and different HDPE/wax/Cu microcomposites. [Color figure can be viewed in the online issue, which is available at www.interscience.wiley.com.]

the decrease was probably the result of wax-covered Cu particles that formed defect centers in the amorphous phase of the polymer. The poor mechanical properties of the wax as well as the fact that the wax seemed to have weaker interactions with the polymer than Cu (the mechanical behavior of composites depends on the quality of adhesion between the matrix and filler, and in this case, the filler was wax-covered Cu particles) also contributed to the observed decrease in the tensile strength with increasing Cu content. According to Nielsen[27] and Kunori and Geil[28] strong interfacial adhesion between the dispersed and continuous phases produces a high stress at break in the composite. The HDPE/wax/Cu composites showed very little change in the tensile strength with increasing Cu content and were similar in this way to the HDPE/Cu microcomposites.[29] Because the filler was located only in the amorphous phase, the concentration of the filler with respect to the amorphous content was higher in HDPE. The result of this was that the amorphous part in the more crystalline polymer (HDPE) was more reinforced in comparison with the relatively low-crystallinity polymer (LDPE) because of a higher local concentration of the filler in the amorphous phase. Orientational hardening of the polymer matrix also contributed to a decrease in the tensile strength of the composite. The smallest decrease in the tensile strength was observed for LDPE and HDPE, whereas no orientational hardening was even observed for the pure polymer. In all these cases, no reinforcing effect of the filler was observed.

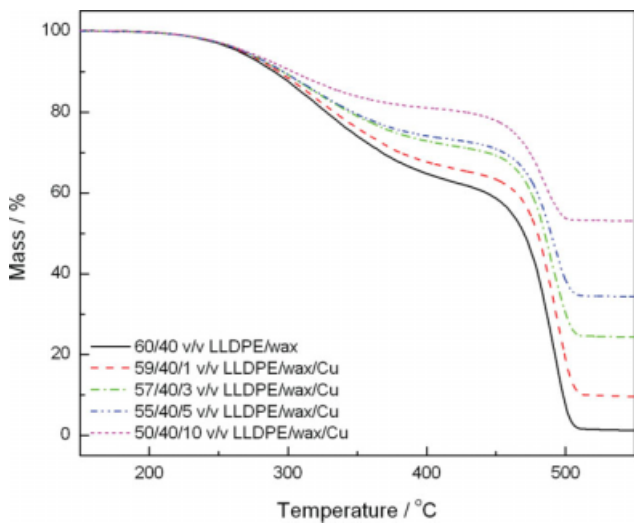

Figure 6 TGA curves for the LLDPE, wax, and different LLDPE/wax/Cu microcomposites. [Color figure can be viewed in the online issue, which is available at www.interscience.wiley.com.]

The dependence of the elongation at break on the Cu content in the blend composites is summarized in Table III. The observed trends were the same as those for the stress at break and may be explained in a similar way. Young's modulus of the PE/wax/Cu composites as a function of the Cu content with 40 vol % wax is summarized in Table III. Young's modulus increased with an increase in the filler content at a constant wax concentration for the LDPE/wax/Cu and LLDPE/wax/Cu composites, but it slightly decreased for the HDPE/wax/Cu composites. The reason for the drop in Young's modulus of the HDPE/wax/Cu microcomposites was probably the insufficient interaction between HDPE and the wax-covered Cu particles, which increased the chain mobility in the vicinity of the filler. The values were

TABLE II
Temperatures of 10, 20, and 50% Degradation (T_{10}, T_{20}, and T_{50}, Respectively) of the PE/Wax/Cu Microcomposites

v/v	T_{10} (°C)	T_{20} (°C)	T_{50} (°C)	Residue (wt %)	Cu in the sample (wt %)
LDPE/wax/Cu					
60/40/0	282.4	313.4	439.4	0.0	0.0
59/40/1	289.9	326.9	470.9	7.8	7.0
57/40/3	293.0	334.0	477.0	21.5	23.6
55/40/5	292.8	337.8	478.8	30.4	33.9
50/40/10	298.3	354.3	—	41.8	42.0
LLDPE/wax/Cu					
60/40/0	282.4	327.1	469.1	0.0	0.0
59/40/1	292.7	329.7	479.7	9.7	8.7
57/40/3	295.9	339.9	484.9	24.4	24.0
55/40/5	295.9	341.9	488.9	34.4	34.0
50/40/10	303.0	427.0	—	53.1	51.0
HDPE/wax/Cu					
60/40/0	294.8	340.8	478.8	0.0	0.0
59/40/1	294.7	333.7	478.7	9.1	8.9
57/40/3	289.2	329.2	484.2	22.7	21.0
55/40/5	292.8	340.2	487.2	31.7	30.3
50/40/10	298.3	404.0	—	53.7	51.9

higher for the LLDPE matrices than for the LDPE matrices. This was in line with the known crystallinities of the respective PEs. The HDPE composites had higher Young's modulus values than the LDPE and LLDPE composites because of the higher crystallinity of HDPE.

TABLE III
Mechanical Properties of the PE/Wax/Cu Microcomposites

v/v	$\sigma_b \pm S\sigma_b$ (MPa)	$\varepsilon_b \pm S\varepsilon_b$ (%)	$E \pm sE$ (MPa)
LDPE/wax/Cu			
60/40/0	9.1 ± 0.6	19.0 ± 9.4	185 ± 12
59/40/1	9.4 ± 0.1	20.6 ± 0.1	183 ± 11
57/40/3	8.9 ± 0.2	16.8 ± 0.4	207 ± 1
55/40/5	8.4 ± 0.2	11.4 ± 2.9	179 ± 3
50/40/10	6.8 ± 0.9	4.3 ± 1.2	271 ± 19
45/40/15	4.7 ± 1.4	3.6 ± 1.1	226 ± 33
LLDPE/wax/Cu			
60/40/0	8.4 ± 0.9	570 ± 18	166 ± 5
59/40/1	10.4 ± 2.0	683 ± 84	149 ± 5
57/40/3	9.4 ± 0.2	532 ± 29	169 ± 7
55/40/5	7.7 ± 0.3	524 ± 46	193 ± 6
50/40/10	7.0 ± 0.1	153.5 ± 5.9	199 ± 10
45/40/15	7.1 ± 3.1	13.7 ± 3.1	250 ± 18
HDPE/wax/Cu			
60/40/0	8.6 ± 4.1	247 ± 140	325 ± 42
59/40/1	8.1 ± 5.5	35.7 ± 4.1	353 ± 31
57/40/3	10.0 ± 4.8	27.8 ± 4.1.	354 ± 32
55/405	10.2 ± 2.7	15.5 ± 8.1	351 ± 1
50/40/10	11.1 ± 0.6	14.8 ± 4.4	304 ± 18
45/40/15	9.0 ± 1.0	10.4 ± 4.7	300 ± 8

σ_b = stress at break; $S\sigma_b$ = standard deviation of the stress at break; ε_b = elongation at break; $S\varepsilon_b$ = standard deviation of the elongation at break; E = Young's modulus; sE = standard deviation of Young's modulus.

Thermal conductivity

The thermal conductivity of all the investigated blend composites initially decreased with a Cu particle concentration of 1 vol % at a constant wax concentration 40 vol % (Fig. 8). A further increase in the Cu content led to a nonlinear increase in the thermal conductivity of these composites. The initial decrease in the thermal conductivity could have been caused by voids formed at the interface between the polymer and the wax (Fig. 1). These voids were filled by air, which decreased the thermal conductivity. The thermal conductivity of the PE/wax/Cu

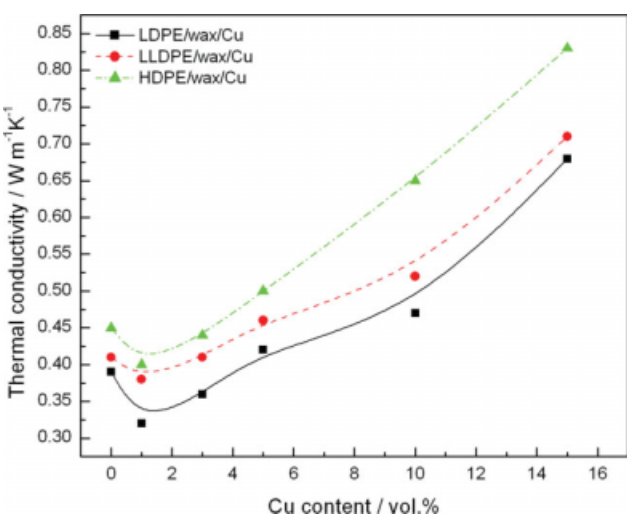

Figure 8 Thermal conductivities of the PE/wax/Cu microcomposites. [Color figure can be viewed in the online issue, which is available at www.interscience.wiley.com.]

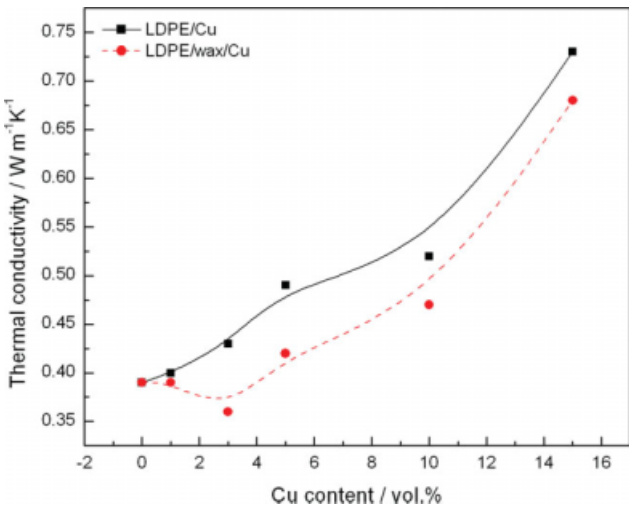

Figure 9 Comparison of the thermal conductivities of the LDPE/Cu and LDPE/wax/Cu microcomposites. [Color figure can be viewed in the online issue, which is available at www.interscience.wiley.com.]

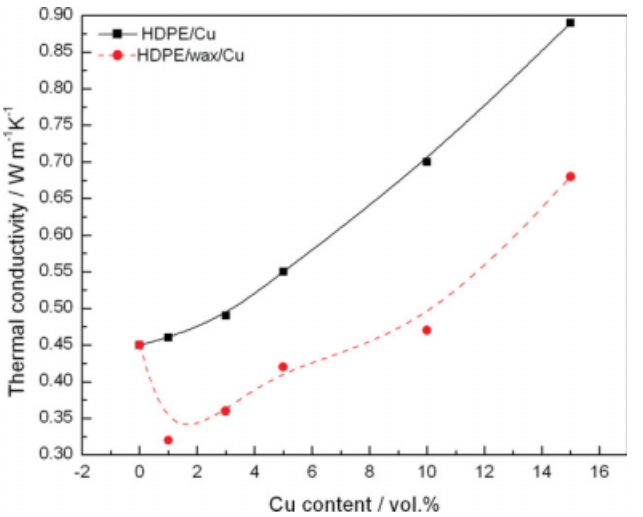

Figure 11 Comparison of the thermal conductivities of the HDPE/Cu and HDPE/wax/Cu microcomposites. [Color figure can be viewed in the online issue, which is available at www.interscience.wiley.com.]

microcomposites was lower than that of the PE/Cu microcomposites (Figs. 9–11). Because the wax seemed to be concentrated around the Cu particles, it isolated the conductive particles from the PE. It was known that the wax (0.24 W m^{-1} K^{-1}) had lower conductivity than the PEs (0.39 W m^{-1} K^{-1}), and this explained the lower thermal conductivity of the blend composites.

The Cu microparticles improved the thermal conductivity of the PCMs by about 50–70%, and this was dependent on the type of PE. One could expect further increases in the thermal conductivity of the materials with an increase in the filler content. However, there must be a compromise between the concentrations of all the components, that is, the polymer, wax, and Cu particles. A further increase in the filler content could happen only at the expense of the polymer or wax contents. However, a decrease in the polymer content would result in a loss of material compactness (the polymer binds all the components together), whereas a decrease in the wax content would lead to a decrease in the heat absorption efficiency. This fact must always be taken into account when PCMs are designed.

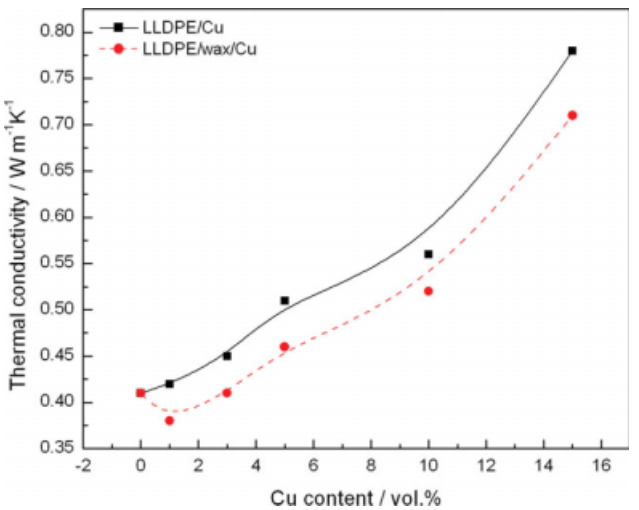

Figure 10 Comparison of the thermal conductivities of the LLDPE/Cu and LLDPE/wax/Cu microcomposites. [Color figure can be viewed in the online issue, which is available at www.interscience.wiley.com.]

CONCLUSIONS

Introducing Cu microparticles into PCMs based on different PEs and a soft Fischer-Tropsch paraffin wax did not significantly change the crystallization behavior, thermal stability, or tensile properties of the blend composites in comparison with the corresponding PE/wax blends and PE/Cu composites. The observed differences were related to the fact that the wax seemed to have a higher affinity for the Cu particles than any of the PEs; therefore, it crystallized as a layer around the Cu particles. The thermal conductivity of the samples increased almost linearly with increasing Cu content, but the samples had slightly lower values than the corresponding PE/Cu composites, probably because of the lower thermal conductivity of the wax. Nevertheless, it seems as if the presence of Cu microparticles in a phase-change PE/wax blend will improve the thermal conductivity of the material without adversely affecting its crystallinity, thermal stability, or mechanical properties.

References

1. Khudhair, A. M.; Farid, M. M. Energy Convers Manage 2004, 45, 263.
2. Hasnain, S. M. Energy Convers Manage 1998, 39, 1127.
3. Zalba, B.; Marin, J. M.; Cabeza, L. F.; Mehling, H. Appl Therm Eng 2003, 23, 251.
4. Elgafy, A.; Lafdi, K. Carbon 2005, 43, 3067.
5. Zhang, Z.; Fang, X. Energy Convers Manage 2006, 47, 303.
6. Hong, Y.; Xin-Shi, G. Sol Energy Mater Sol Cells 2000, 64, 37.
7. Asinger, F. Paraffins: Chemistry and Technology; Pergamon: Elmsford, NY, 1967.
8. Cai, Y.; Hu, Y.; Song, L.; Tang, Y.; Yang, R.; Zhang, Y.; Chen, Z.; Fan, W. J Appl Polym Sci 2006, 99, 1320.
9. Xiao, M.; Feng, B.; Gong, K. Energy Convers Manage 2002, 43, 103.
10. Gschwander, S.; Schossig, P.; Henning, H. M. Sol Energy Mater Sol Cells 2005, 89, 307.
11. Wang, W.; Yang, X.; Fang, Y.; Ding, J.; Yan, J. Appl Energy 2009, 86, 1479.
12. Li, J.; Xue, P.; Ding, W.; Han, J.; Sun, G. Sol Energy Mater Sol Cells, to appear.
13. Wang, J.; Xie, H.; Xin, Z. Thermochim Acta 2009, 488, 39.
14. Wang, W.; Yang, X.; Fang, Y.; Ding, J.; Yan, J. Appl Energy 2009, 86, 1196.
15. Mazman, M.; Cabeza, L. F.; Mehling, H.; Paksoy, H. Ö.; Evliya, H. Int J Energy Res 2008, 32, 135.
16. Salyer, I. O. U.S. Pat. 5,565,132 (1996).
17. Xiao, M.; Feng, B.; Gong, K. Sol Energy Mater Sol Cells 2001, 69, 293.
18. Inaba, H.; Tu, P. Heat Mass Transfer 1997, 32, 307.
19. Hong, Y.; Xin-Shi, G. Sol Energy Mater Sol Cells 2000, 64, 37.
20. Sari, A. Energy Convers Manage 2004, 45, 2033.
21. Krupa, I.; Luyt, A. S. Polym Degrad Stab 2000, 70, 111.
22. Mtshali, T. N.; Krupa, I.; Luyt, A. S. Thermochim Acta 2001, 380, 47.
23. Luyt, A. S.; Krupa, I. Macromol Symp 2002, 178, 109.
24. Krupa, I.; Miková, G.; Luyt, A. S. Eur Polym J 2007, 43, 4695.
25. Krupa, I.; Miková, G.; Luyt, A. S. Eur Polym J 2007, 43, 895.
26. Molefi, J. A.; Luyt, A. S.; Krupa, I. Thermochim Acta, to appear.
27. Nielsen, L. E. Mechanical Properties of Polymers and Composites; Marcel Dekker: New York, 1974.
28. Kunori, T.; Geil, P. J Macromol Sci Phys 1980, 18, 135.
29. Molefi, J. A.; Luyt, A. S.; Krupa, I. eXPRESS Polym Lett 2009, 3, 639.